

## Colloid Properties of Paramagnetic Nanoparticles Based on Novel Thiocalix[4]arenes and Gd(III) Ions

Alexey S. Stepanov,<sup>@</sup> Svetlana E. Solovieva, Aidar T. Gubaidullin,  
and Asiya R. Mustafina

*A.E. Arbuzov Institute of Organic and Physical Chemistry, Kazan Scientific Center, Russian Academy of Sciences, 420088 Kazan, Russia*

<sup>@</sup>Corresponding author E-mail: [aleksestepanov@yandex.ru](mailto:aleksestepanov@yandex.ru)

*The present work introduces colloid behaviour of core-shell nanoparticles, where hard paramagnetic cores are coated by hydrophilic polyelectrolyte-based shells. Paramagnetic cores are built from water insoluble Gd(III) complexes with alkyl-malonate derivatives of thiocalix[4]arenes adopting 1,3-alternate conformation. Polystyrenesulfonate (PSS) and polyethyleneimine (PEI) are used to deposit one (PSS) or two (PSS-PEI) polyelectrolyte layers onto the cores. Small angle light scattering was used to reveal both size and aggregation behaviour of the core-shell colloids in aqueous solutions.*

**Keywords:** Malonate thiocalix[4]arenes, colloids, small angle X-Ray scattering, Gd(III) ions.

## Коллоидные свойства парамагнитных наночастиц на основе новых тиакаликс[4]аренов и ионов Gd(III)

А. С. Степанов,<sup>@</sup> С. Е. Соловьёва, А. Т. Губайдуллин, А. Р. Мустафина

*Институт органической и физической химии им. А.Е. Арбузова Казанского научного центра Российской академии наук, 420088 Казань, Россия*

<sup>@</sup>E-mail: [aleksestepanov@yandex.ru](mailto:aleksestepanov@yandex.ru)

*Настоящая работа представляет коллоидные свойства наночастиц морфологии ядро-оболочка, в которых твёрдые парамагнитные ядра заключены в гидрофильную полиэлектролитную оболочку. Парамагнитные ядра состоят из водонерастворимых комплексов гадолиния с алкил-малонатными тиакаликс[4]аренами в конформации 1,3-альтернат. Для осаждения твёрдых ядер использовался полистиролсульфонат (PSS) и полиэтиленимин (PEI). Размер и агрегационное поведение полученных водных коллоидов полиэлектролитных наночастиц были изучены методом малоуглового рентгеновского рассеяния.*

**Ключевые слова:** Малонатные тиакаликс[4]арены, коллоиды, малоугловое рентгеновское рассеяние, ионы Gd(III).

## Introduction

Gd(III) complexes have attracted significant attention of researches in recent decades owing to their use in magnetic resonance imaging (MRI).<sup>[1-3]</sup> A great number of commercial MRI contrast agents are based on Gd(III) complexes.<sup>[1,3]</sup> It must be mentioned that longitudinal relaxivity and stability of molecular contrast agents can be easily tuned by variation of hydration number and ligands of Gd(III). Nevertheless, the drawbacks of the molecular complexes, such as toxicity and adverse effects, provoked the development of nanoparticulate approach, where nanosized species of water insoluble salts,<sup>[4-12]</sup> oxides<sup>[13-24]</sup> or complexes<sup>[25,26]</sup> of Gd(III) are stabilized with polyethyleneoxides or poly-electrolytes. Literature data indicate main factors affecting magnetic relaxation rates in aqueous dispersions of Gd(III) nanoparticles, although no proper theory for accurate interpretation of relaxivities in Gd(III)-based colloids is available to date. It is well-known that nanoparticulate form of Gd(III) complexes increase longitudinal relaxivity due to slowed down translational movement of Gd(III) centres.<sup>[27-28]</sup> The size of nanoparticles greatly affects the relaxivity. In particular, the size should be about 2 nm for successful hydration of the majority of Gd(III) centres within nanoparticles.<sup>[29-31]</sup> Thus, any external factors guiding a transformation of Gd(III) complexes into Gd(III)-based nanoparticles are of great importance in improving of longitudinal relaxivity. From this point of view Gd(III) complexes are more suitable for phase and size optimization through changing their water solubility than Gd(III)-based nanoparticles.

Coordination chemistry of lanthanide complexes with polycarbonic acids demonstrates many examples, where precipitated electroneutral complex tends to dissolve upon further deprotonation of carboxylic groups, which are not participated in coordination with Gd(III).<sup>[32]</sup> It must be added that the development of nanoparticulate Gd(III) contrast agents requires specific solubility of Gd(III) complexes. The solubility should be rather poor to form hard Gd(III)-containing dispersions, but not too poor to avoid their uncontrollable growth. Ligands with hydrophilic chelating groups embedded to hydrophobic macrocyclic backbone, such as calix[4]arene, calix[4]resorcinarene or thiacalix[4]arene are well-known versatile platforms for metal complexes.<sup>[33-35]</sup> For example, Schühle *et al.* has reported Gd-DOTA complexes conjugated with calix[4]arene possessing high longitudinal relaxivity of 31.2 mM<sup>-1</sup>·s<sup>-1</sup>.<sup>[36]</sup>

In our previous paper we have reported the pH-dependent complex formation of Gd(III) ions *via* novel alkyl-malonate thiacalix[4]arenes substituents in H<sub>2</sub>O-DMSO solutions. The precipitated complexes have been converted into hydrophilic colloids of “plum-pudding” morphology, where the Gd(III) complexes form hard small (1.5–4 nm) cores included into larger (about 180 nm) soft PSS shells. The obtained colloids have demonstrated high longitudinal and transverse relaxivities ( $r_1=23.8$  and  $r_2=29.4$  mM<sup>-1</sup>·s<sup>-1</sup> at 0.47 T, respectively). The DLS study revealed the average sizes and electrokinetic potentials of the colloids. However, DLS does not allow for detection of the hard cores of the colloids. In view of the aforesaid, in the present article we have thoroughly investigated the colloidal properties of these nanoparticles by means of small-angle X-ray scattering (SAXS).

## Experimental

### Materials

Commercial chemicals Gd(NO<sub>3</sub>)<sub>3</sub>·6H<sub>2</sub>O (99.9 %), K<sub>2</sub>CO<sub>3</sub> (99.9 %), NaOH (pellets, 98.5 %), KOH (pellets, 98.5 %), HNO<sub>3</sub> (70 %), HCl (37 %), H<sub>2</sub>SO<sub>4</sub> (96 %), dimethylsulfoxide (DMSO) (99.8 %), dimethylformamide (DMF) (99 %), chloroform (99.9 %), NaH (60 % suspension in oil), MgSO<sub>4</sub> (99 %), glacial acetic acid (99 %), xylene orange (*o*-cresolsulphonphthaleindi-(methyliminodiacetic acid) sodium salt), poly(sodium-*p*-styrenesulfonate) (Mw ~70000) were obtained from Acros Organics. Malonic ether was purchased from Alfa Aesar (99 %). Deuterated chloroform and (99.8 %), DMSO (99.8 %), polyethylenimine (PEI) (Mw ~25000) were purchased from Sigma Aldrich. DMSO and DMF were distilled twice over P<sub>2</sub>O<sub>5</sub> under reduced pressure prior to use. Chloroform was purified as follows: a certain volume of CHCl<sub>3</sub> was washed a few times with doubly distilled water and concentrated H<sub>2</sub>SO<sub>4</sub>, dried over K<sub>2</sub>CO<sub>3</sub> and finally was distilled at atmospheric pressure. All other chemicals were used as received without further purification.

The synthesis of thiacalix[4]arenes outlined in Scheme 1 has been reported by us previously.<sup>[37]</sup>

### Synthesis of PSS and PSS-PEI-stabilized aqueous colloids

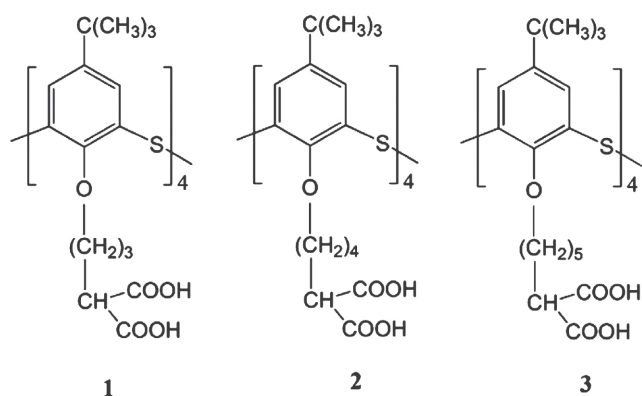
A series of DMSO solutions containing different concentrations of ligands **1**, **2**, **3** (1.2·10<sup>-3</sup> M) and Gd(NO<sub>3</sub>)<sub>3</sub> (1.2·10<sup>-3</sup> M) at various concentrations of Et<sub>3</sub>N have been prepared. Et<sub>3</sub>N was varied to be at 1:1, 1:2, 1:4, 1:6, 1:8, 1:10, 1:12 ligand:Et<sub>3</sub>N concentrations ratios. After that 1 ml of solution containing Gd(III), calixarene and Et<sub>3</sub>N has been added dropwise with the help of syringe pump (adding rate 1 mL·min<sup>-1</sup>) to the 5 ml of aqueous solution of PSS (1 g·L<sup>-1</sup>, 0.5 M NaCl) under vigorous stirring (1400 rpm). The prepared aqueous-DMSO solution was then sonicated for 30 minutes with use of ultrasound water bath and centrifuged (13500 rpm, 20 min). The separated colloids were then washed with doubly distilled water by four centrifugation/redispersion steps.

### Determination of Gd(III) concentration in the obtained colloids

After being washed with water the real concentration of Gd(III) in the obtained suspensions was determined as follows: 50 μL of 1M HNO<sub>3</sub> were added to 6 mL of the studied suspension and shaken vigorously for 1 min to yield virtually transparent solution. Then this solution was analyzed for Gd(III) quantity spectrophotometrically with use of Xylene Orange.

### Methods

Small angle X-Ray scattering (SAXS) data for samples were collected with the Bruker AXS Nanostar SAXS system using CuK<sub>α</sub> (λ 1.5418 Å) radiation from a 2.2 kW X-ray tube (35 kV, 40 mA) coupled with Gobbel mirrors optics and a HiStar 2D area detector. The beam was collimated using three pinholes with apertures of 800, 450 and 700 μm. The instrument was operated with a sample-to-detector distance of 63.5 cm to provide data at angles 0.1° < 2θ < 4.8°, which correspond to 0.007 Å<sup>-1</sup> < q < 0.34 Å<sup>-1</sup>. The value of q is proportional to the inverse of the length scale ( $q=(4\pi/\lambda)\sin(\theta)$  in units of Å<sup>-1</sup>). Scattering patterns were obtained for the samples at 23 °C in an evacuated chamber. The measurements were performed in transition mode with the use of 2 mm glass capillaries filled by liquid samples. Two experiments at least were performed for each sample in order to control the quality. The results of two experiments are summarized, so that the total time of each



**Scheme 1.** Structures of the ligands **1**, **2**, **3**.

experiment was equal to 50000 s. Integration of two-dimensional pictures scattering was performed using a software package SAXS [Small Angle X-ray Scattering. Version 4.0. Software Reference Manual, 2000, M86-E00005-0600, Bruker AXS Inc.].

*pH* values of the solutions were controlled with Microprocessor *pH* meter «*pH* 212» (Hanna Instruments, Germany) The *pH*-meter was calibrated with standard aqueous buffer solutions (*pH* 7.01 and 4.01).

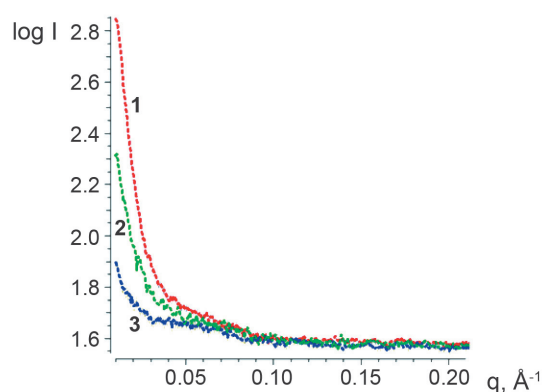
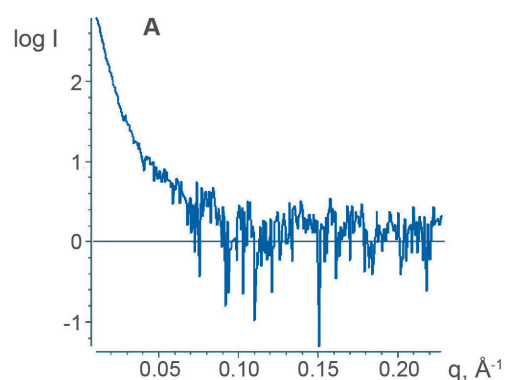


**Figure 1.** The experimental SAXS curves of PSS- $[\text{Gd}_x(\mathbf{1})_y]$  colloid (1),  $[\text{Gd}_x(\mathbf{1})_y]$  colloid (2) and water (3) in glass 2 mm capillaries, in logarithmic ( $\log I$  vs.  $q$ ) scale.



## Results and Discussion

As mentioned in our earlier paper the good solubility of thiocalix[4]arenes **1**, **2**, **3** was found in DMSO<sup>[37]</sup> and it was used as the solvent for complex formation with Gd(III). Triethylamine (TEA) was added to deprotonate malonic acid moieties for further binding with Gd(III) ions. Then, the dropwise addition of Gd(III) complexes with thiocalix[4]arenes in DMSO to aqueous solution of PSS (0.5 M NaCl) precipitates the complexes in the form of hard cores followed by their stabilization with PSS. The detailed synthetic procedure to obtain PSS and PSS-PEI-stabilized colloids is described in detail in the experimental section of the article. From now on, the corresponding colloids are called after the following abbreviations:  $[\text{Gd}_x(\mathbf{1})_y]$ ,  $[\text{Gd}_x(\mathbf{2})_y]$ ,  $[\text{Gd}_x(\mathbf{3})_y]$  signify unstabilized particles, whereas PSS-(PEI)- $[\text{Gd}_x(\mathbf{1,2,3})_y]$  stand for polyelectrolyte-stabilized ones.

To obtain additional information about colloid properties of the nanoparticles in aqueous solutions, two samples –  $[\text{Gd}_x(\mathbf{1})_y]$  colloid and PSS-stabilized  $[\text{Gd}_x(\mathbf{1})_y]$  colloid – were carefully investigated by SAXS method. Integration of the 2D diffraction patterns yielded diffraction profiles of small-angle scattering from the samples. For comparison, Figure 1 shows the diffraction patterns of the scattering from water and from the samples without background subtraction. The rather high scattering intensity indicates the heterogeneity of the samples – the presence of the randomly oriented particles in solutions, the dimensional characteristics of which correspond to the information area of the SAXS method (1–100 nm).<sup>[38]</sup>

Scattering curves resulted from the subtraction of the buffer (scattering of water in glass capillary) from the samples, are presented in Figure 2.

Power law slopes from the data in the high- $q$  region can be used to describe the morphology of the system. One of the important features deduced from power law slopes is the radius of gyration ( $R_g$ ).<sup>[38]</sup> This size parameter, the radius of gyration, is the square root of the average squared distance of each scatterer from the particle centre. For two samples, these parameters calculated by two different methods based on data analysis in direct and reciprocal space.<sup>[39,40]</sup> Additionally, we used PRIMUS program<sup>[41]</sup> for the fitting of small-angle X-ray scattering spectra in a globular model

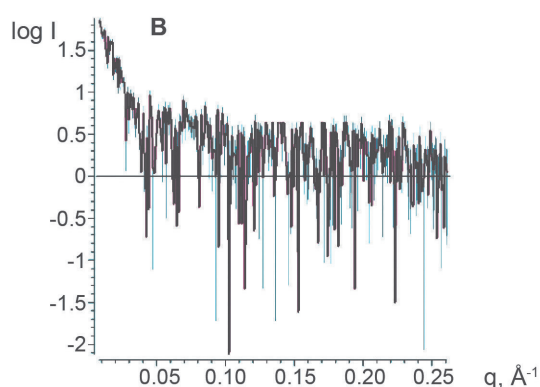


**Figure 2.** The experimental SAXS curves of (A) PSS- $[\text{Gd}_x(\mathbf{1})_y]$  colloid and (B)  $[\text{Gd}_x(\mathbf{1})_y]$  colloid after background subtraction, in logarithmic ( $\log I$  vs.  $q$ ) scale.

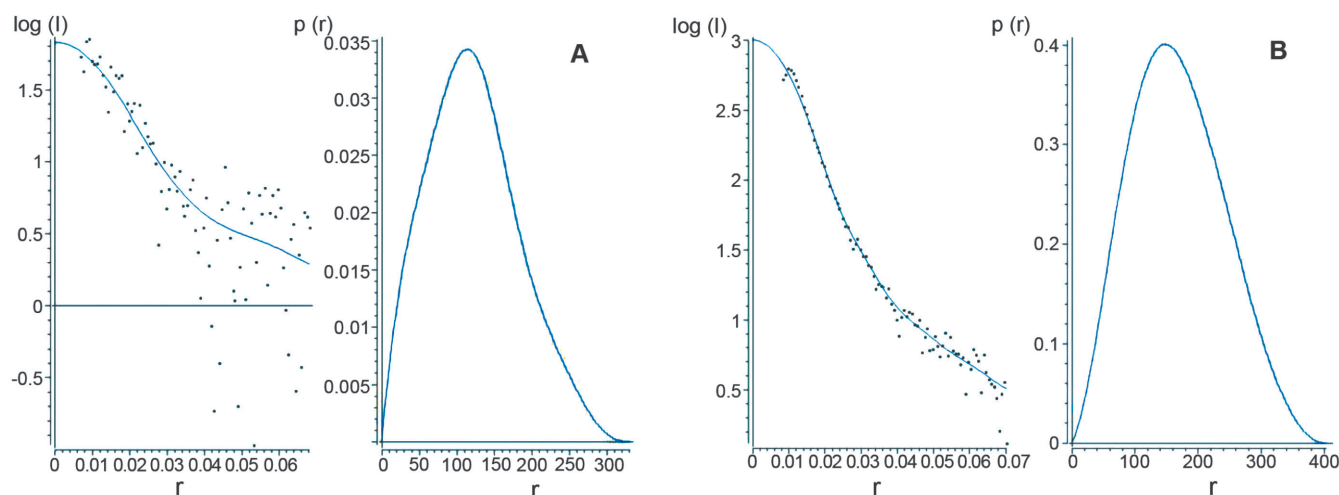


**Figure 3.** The fitting of experimental SAXS curves (points – experimental data, curves – simulation) and calculated distance distribution functions  $p(r)$  for PSS-[Gd<sub>x</sub>(1)<sub>y</sub>] colloid (a) and [Gd<sub>x</sub>(1)<sub>y</sub>] colloid (b).

with a local monodisperse approximation and calculated the distance distribution function  $p(r)$  in the particles (Figure 3).

A fit of the data for [Gd<sub>x</sub>(1)<sub>y</sub>] colloid gave the following parameters: reciprocal space radius of gyration  $R_g$  96.7 Å, real space  $R_g = 96.92 \pm 2.93$  Å, the maximum characteristic size in the particle  $D_{\max}$  331.4 Å, Porod volume  $2.90 \cdot 10^6$  Å<sup>3</sup>. For PSS-stabilized [Gd<sub>x</sub>(1)<sub>y</sub>] colloid the reciprocal space radius of gyration  $R_g$  is 130.0 Å, real space  $R_g = 129.9 \pm 1.2$  Å, the maximum characteristic size in the particle  $D_{\max}$  is 404.3 Å, and Porod volume is  $9.26 \cdot 10^6$  Å<sup>3</sup>. The values of radius of gyration obtained by two methods are generally quite close and, in the case of sphere-shaped model, corresponds to the effective radius of the particles 167.6 Å and 125.1 Å for PSS-stabilized [Gd<sub>x</sub>(1)<sub>y</sub>] colloid and [Gd<sub>x</sub>(1)<sub>y</sub>] colloid, respectively.

Thus, a comparison of the data obtained indicates a significant increase in the [Gd<sub>x</sub>(1)<sub>y</sub>] colloid particles radius during their PSS stabilization, which is apparently due to the enveloping of the particle core by the PSS molecules. This leads to a corresponding increase in the particle size and volume. In this case, comparing the values of the calculated effective particle radii (assuming their sphericity) with the values of the maximum distance  $D_{\max}$  in the particles makes it possible to conclude that for both samples the deviation of the shape of the particle from spherical to globular (or ellipsoidal) form is observed.

The  $R_g$  value for PSS-PEI-[Gd<sub>x</sub>(1)<sub>y</sub>] colloids is  $86.58 \pm 0.96$  Å. This result disagrees with the thickening of the polyelectrolyte-based exterior layer, but agrees well with the partial dissolution of the hard cores revealed in our previous work. The similar  $R_g$  value is revealed for PSS-PEI-[Gd<sub>x</sub>(2)<sub>y</sub>] colloids (129.7 Å), the maximum characteristic size in the particle  $D_{\max}$  401.4 Å, and Porod volume  $7.79 \cdot 10^6$  Å<sup>3</sup>. The increased basicity of the microenvironment of the hard cores is the reason for dissolution of the hard cores due to deprotonation of the polycarboxylate Gd(III) complexes.

Indeed, for [Gd<sub>x</sub>(3)<sub>y</sub>], PSS-[Gd<sub>x</sub>(3)<sub>y</sub>] and PSS-PEI-[Gd<sub>x</sub>(3)<sub>y</sub>] colloids  $R_g$  values are 41.8 Å, 90.9 Å, 94.4 Å, respectively, with the latter colloid having  $D_{\max} = 262$  Å,

Porod volume  $2.89 \cdot 10^5$  Å<sup>3</sup>. The size decrease is in good confirmation with the previously reported tendency, which reveals significant effect of the ligand structure on water solubility of the Gd(III) complexes. Taking into account the great impact of the water insolubility of Gd(III) complexes with alkyl-malonate-substituted thiacalix[4]arenes in the formation of the PSS-stabilized colloids the tendency revealed by SAXS measurements is in good agreement with the previously reported decrease in the colloid concentration on going from PSS-[Gd<sub>x</sub>(1)<sub>y</sub>] and PSS-[Gd<sub>x</sub>(2)<sub>y</sub>] to PSS-[Gd<sub>x</sub>(3)<sub>y</sub>]. It is also worth noting that the sizes evaluated by SAXS are in good agreement with the earlier reported electronic microscopy images, while much smaller than the sizes measured by dynamic light scattering (DLS) technique. Moreover, the previously reported DLS results did not differentiate between the colloids, while the difference in the turbidity of the colloids was revealed by the spectrophotometry results. Thus, SAXS procedure provides much more reliable colloid properties than DLS for aqueous core-shell colloids.

## Conclusions

The work introduces colloid properties of Gd(III)-based aqueous core-shell colloids built from water insoluble propyl-malonate-substituted thiacalix[4]arene adopting 1,3-alternate conformation and Gd(III) ions facilitated by polystyrolsulfonate (PSS). The small angle light scattering data are represented herein as powerful tool to evaluate size of the Gd(III)-based cores coated by polyelectrolyte-based mono- and bi-layer. The presented herein experimental data confirm the significant effect of the polyelectrolyte-based shell on the size of the hard cores resulted from their dissolution, which in turn derives from increased basicity of the hard cores microenvironment. Moreover, the structure of alkyl-malonate-substituted thiacalix[4]arene, in particular, a length of the alkyl-linker is another reason for the effect on the colloids properties. The good agreement between the tendencies revealed from small angle X-ray scattering data

with the previously reported electronic microscopy images and concentration of the paramagnetic colloids highlights the SAXS as convenient procedure to reveal size, shape and aggregation behaviour of the paramagnetic core-shell colloids in aqueous solutions.

**Acknowledgements.** We thank RSF (grant no 17-13-01013) for financial support. TEM images were obtained in the laboratory “Transmission electron microscopy” of Kazan National Research Technological University.

## References

- Burtea C., Laurent S., Elst L.V., Muller R.N. *Handbook of Experimental Pharmacology* **2008**, 185 (PART 1), 135–165.
- Lauffer R.B. *Chem. Rev.* **1988**, 87, 901–927.
- Platzek J., Blaszkiewicz P., Gries H., Luger P., Mishl G., Muller-Fahnow A., Raduchel B., Sulzle D. *Inorg. Chem.* **1997**, 36, 6086–6093.
- Na H.B., Song I.C., Hyeon T. *Adv. Mater.* **2009**, 21, 2133–2148.
- Na H.B., Lee J.H., An K., Park Y.I., Park I.S., Nam D.-H., Kim S.T., Kim S.-H., Kim S.-W., Lim K.-H., Kim K.-S., Kim S.-O., Hyeon T. *Angew. Chem. Int. Ed.* **2007**, 46, 5397.
- Hifumi H., Yamaoka S., Tanimoto A., Citterio D., Suzuki K. *J. Am. Chem. Soc.* **2006**, 128, 15090.
- Evanics F., Diamante P.R., van Veggel F.C.J.M., Stanis G.J., Prosser R.S. *Chem. Mater.* **2006**, 18, 2499.
- Xu X., Zhang X., Wu Y. *J. Nanopart. Res.* **2016**, 11, 334–335.
- Zhou J., Sun Y., Du X.X., Xiong L.Q., Hu H., Li F.Y. *Biomaterials* **2010**, 31, 3287–3295.
- Dong K., Ju E.G., Liu J.H., Han X.L., Ren J.S., Qu X.G. *Nanoscale* **2014**, 6, 12042–12049.
- Rodriguez-Liviano S., Becerro A.I., Alcantara D., Grazu V., Fuente J.M.D.L., Ocana M. *Chem. Inform.* **2013**, 44, 647–654.
- Ren W.L., Tian G., Zhou L.J., Yin W.Y., Yan L., Jin S., Zu Y., Li S.J., Gu Z.J., Zhao Y.L. *Nanoscale* **2012**, 4, 3754–3760.
- Zhou C.H., Wu H., Huang C.S., Wang M.L., Jia N.Q. *Part. Part. Syst. Char.* **2014**, 31, 675–684.
- Majeed S., Shivashankar S.A. *J. Mater. Chem. B* **2014**, 2, 5585–5593.
- Bridot J.-L., Faure A.-C., Laurent S., Riviere C., Billotey C., Hiba B., Janier M., Josserand V., Coll J.-L., Elst L.V., Muller R., Roux S., Perriat P., Tillement O. *J. Am. Chem. Soc.* **2007**, 129, 5076–5084.
- Wang F., Peng E., Zheng B., Fong S., Li S.F.Y., Xue J.M. *J. Phys. Chem. C* **2015**, 119, 23735–23742.
- Park J.Y., Baek M.J., Choi E.S., Woo S., Kim J.H., Kim T.J., Jung J.C., Chae K.S., Chang Y., Lee G.H. *ACS Nano* **2009**, 3, 3663–3669.
- Luo N.Q., Tian X.M., Yang C., Xiao J., Hu W.Y., Chen D.H., Li L. *Chem. Chem. Phys.* **2013**, 15, 12235–12240.
- Cho M., Sethi R., Narayanan J.S.A., Lee S.S., Benoit D.N., Taheri N., Decizzi P., Colvin V.L. *Nanoscale* **2014**, 6, 13637–13645.
- Chen J., Shi Y., Shi J. *J. Mater. Res.* **2004**, 19, 3586–3591.
- Fang J., Chandrasekharan P., Liu X.L., Yang Y., Lv Y.B., Yang C.T., Ding J. *Biomaterials* **2014**, 35, 1636–1642.
- Li F., Zhi D., Luo Y., Zhang J., Nan X., Zhang Y., Zhou W., Qiu B., Wen L., Liang G. *Nanoscale* **2016**, 8, 12826–12833.
- Babic-Stojic B., Jokanovic V., Milivojevic D., Pozek M., Jaglicic Z., Makovec D., Arsiokin K., Paunovic V. *J. Magn. Magn. Mater.* **2016**, 403, 118–126.
- Gu W., Song G., Li S., Shao C., Yan C., Ye L. *RSC Adv.* **2014**, 4, 50254–50260.
- Aime S., Botta M., Fasano M., Geninatti G.S., Terreno E. *J. Biol. Inorg. Chem.* **1996**, 1, 312–319.
- Morcos S.K. *Eur. J. Radiol.* **2008**, 66, 175–179.
- Perrier M., Kenouche S., Long J., Thangavel K., Larionova J., Goze-Bac C., Lascialfari A., Mariani M., Baril N., Guerin C., Donnadiou B., Trifonov A., Guari Y. *Inorg. Chem.* **2013**, 52, 13402–13414.
- Caravan P., Farrar C.T., Frullano L., Uppal R. *Contrast Media Mol. Biol.* **2009**, 4, 89–100.
- Rieter W.J., Taylor K.M.L., An H., Lin W. *J. Am. Chem. Soc.* **2006**, 128, 9024–9025.
- Pereira G.A., Peters J.A., Almeida Paz F.A., Rocha J., Geraldes C.F.G.C. *Inorg. Chem.* **2010**, 49, 2969–2974.
- Carne-Sanchez A., Bonnet C.S., Imaz I., Lorenzo J., Toth E., MasPOCH D. *J. Am. Chem. Soc.* **2013**, 135, 17711–17714.
- Ramamoorthy S., Manning P.G. *J. Inorg. Nucl. Chem.* **1972**, 34, 1977–1987.
- Shamsutdinova N.A., Gubaidullin A.T., Odintsov B.M., Larsen R.J., Schepkin V.D., Nizameev I.R., Amirov R.R., Zairov R.R., Sudakova S.N., Podyachev S.N., Mustafina A.R., Stepanov A.S. *Chemistry Select* **2016**, 1, 1377–1383.
- Stepanov A.S., Yanilkin V.V., Mustafina A.R., Burilov V.A., Solovieva S.E., Antipin I.S., Konovalov A.I. *Electrochem. Commun.* **2010**, 12, 703–705.
- Sliwa W., Girek T. *J. Inclusion Phenom. Macrocycl. Chem.* **2010**, 66, 15–41.
- Schühle D.T., Polasek M., Lukes I., Chauvin T., Toth E., Schatz J., Hanefeld U., Stuart M.C.A., Peters J.A. *Dalton Trans.* **2010**, 39, 185–191.
- Stepanov A., Nizameev I., Amirov R., Kleshchina S., Khakimulina G., Solovieva S., Voloshina A., Strobaykina A., Gubaidullin A., Nugmanov R., Mustafina A. *Arab. J. Chem.* **2017**, in press.
- Guinier A., Fournet G. *Small-Angle Scattering of X-Rays*. New York: Wiley, **1955**.
- Glatter O. *Small Angle X-Ray Scattering* (Kratky O., Ed.) London: Academic Press, **1982**.
- Feigin L.A., Svergun D.I. *Structure Analysis by Small-Angle X-Ray and Neutron Scattering*. New York: Plenum Press, **1987**.
- Konarev P.V., Volkov V.V., Sokolova A.V., Koch M.H.J., Svergun D.I. *J. Appl. Crystallogr.* **2003**, 36, 1277–1282.

Received 15.05.2017

Accepted 14.06.2017